Inorganic Chemistry

ARTICLE

pubs.acs.org/IC

Yb Valence States in YbC_2: A HERFD-XANES Spectroscopic Investigation

Pascal Link,[†] Pieter Glatzel,[‡] Kristina Kvashnina,[‡] Ronald I. Smith,[§] and Uwe Ruschewitz*[,†]

[†]Department of Chemistry, University of Cologne, Greinstrasse 6, D-50939 Cologne, Germany

[‡]European Synchrotron Radiation Facility, BP 220, 6 rue Horowitz, F-38043 Grenoble, France

[§]ISIS Facility, Rutherford Appleton Laboratory, Chilton, Didcot, Oxfordshire OX11 0QX, U.K.

Supporting Information

ABSTRACT: The valence state of Yb in YbC_2 was analyzed using high-energy-resolution fluorescence detection (HERFD) X-ray absorption near-edge structure (XANES) spectroscopy and time-of-flight neutron powder diffraction to clarify a controversy in the literature. The unit cell volume of YbC_2 suggests a mixed Yb valence, which was formerly determined to be 2.8 by magnetization measurements and paramagnetic neutron scattering techniques. However, the nature of the intermediate valence was not clearly established. Both *homogeneous* and *heterogeneous* mixed valences were assumed in different publications. The temperature-dependent behavior of the valence state was only predicted, albeit not explicitly studied. In this work, the valence state of Yb in YbC_2 is, therefore, investigated thoroughly by HERFD-XANES spectroscopy at low and high temperatures. Our measurements result in an average Yb valence of 2.81 that is temperature-independent from 15 to 1123 K. These findings are confirmed by neutron powder diffraction experiments, which reveal a constant C−C distance of 128.7(9) pm in a temperature range from 5 to 100 K. A significant temperature dependence of the Yb valence state in YbC_2 can, therefore, be excluded by our experimental results.

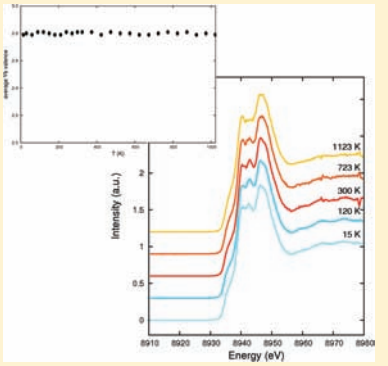

INTRODUCTION

Among the dicarbides of the lanthanide metals LnC_2 (with Ln = La−Lu), YbC_2 is the only compound to date whose cation valence could not be determined clearly. Most of the lanthanide dicarbides contain trivalent cations.[1,2] In a simple picture, they can be described as $Ln^{3+}C_2^{2-}(e^-)$ with a conduction electron delocalized in the conduction band. However, very recently we showed that EuC_2 contains divalent cations and may, therefore, be regarded as the semiconducting species $Eu^{2+}C_2^{2-}$.[3] The divalent state of 2+ is also reflected in the normalized cell volume $V_n = V/Z$ of the compound, which does not follow the usual lanthanide contraction trend. Compared to other LnC_2 compounds, the normalized cell volume of EuC_2 is much too large (Figure 1).

A similar but smaller deviation from the lanthanide contraction trend is observed for YbC_2 (Figure 1). This deviation was already mentioned in the 1950s and 1960s by several authors, who interpreted the effect on the basis of a mixed valence of the Yb ion. Both Atoji[4] and Sales and Wohlleben[5] concordantly reported an intermediate Yb valence of ∼2.8 by interpreting magnetization and paramagnetic neutron scattering data. However, their results differed strongly in the type of model that they used to describe the mixed valence of the compound. Atoji obtained magnetic susceptibilities following the Curie−Weiss law. Consequently, he deduced a *heterogeneous*[6] constant mixed valence without any temperature-dependent fluctuation.[4] At the same time, Sales and Wohlleben did not observe a Curie−Weiss behavior in the magnetic susceptibility data that they measured on YbC_2. Their measurements showed a trend in the susceptibilities that was typical for valence-fluctuating Yb systems. They described the observed susceptibilities by using the ICF (interconfiguration fluctuation) model, deriving a strongly temperature-dependent *homogeneous*[6] Yb valence.[5] Besides paramagnetic neutron scattering experiments, performed by Atoji in 1961,[4] no further experiments using supplementary analytical methods such as Mössbauer or X-ray spectroscopy have been performed from 1973 to date. Thus, it has not been established whether YbC_2 shows a *heterogeneous* or a *homogeneous* mixed valence. Additionally, the temperature dependence of the Yb valence is still ambiguous.

To solve these problems, we determined the Yb valence in YbC_2 by X-ray absorption near-edge structure (XANES) spectroscopy in high-energy-resolution fluorescence detection (HERFD) mode at the Yb L_3 edge. XANES spectroscopy is known as a powerful tool to obtain the valence state of lanthanide metals by determining the energy positions and intensities of the observable white lines at the Ln L_3 edge.[7,8] The white lines of Yb^{2+} and Yb^{3+} are shifted by ∼8 eV; the coexistence of two white lines may therefore be used to identify a mixed-valence state of the Yb ion. By determination of the intensities of the respective lines, it is further possible to calculate the mean valence of the system. However, the spectral features in the conventional XANES experiments are broadened by 4.6 eV at the

Received: February 4, 2011
Published: May 25, 2011

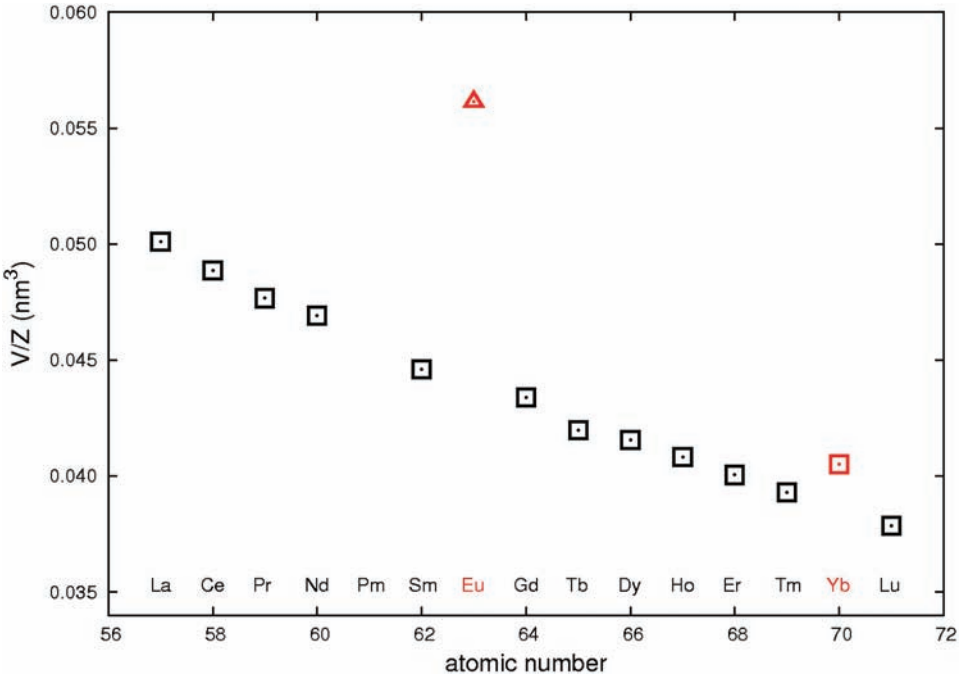

Figure 1. Normalized cell volumes V/Z of the lanthanide dicarbides LnC_2 (⊡, CaC_2-type structure; ⧋, ThC_2-type structure). The volumes of EuC_2 and YbC_2 are highlighted in red because they differ from the remaining compounds.

Table 1. Selected Structural Data of YbC_2 at Room Temperature (Rietveld Refinement, TOF Neutron Powder Diffraction, Polaris/ISIS)[a]

	$\theta \sim 35°$	$\theta \sim 90°$	$\theta \sim 145°$
software		*GSAS*[20]	
space group, Z		*I4/mmm* (No. 139), 2	
a/pm		363.531(3)	
c/pm		611.257(7)	
V/nm^3		0.080780(2)	
atomic coordinates, occupancy, U_{iso} /pm^2			
Yb		2 a 0 0 0, 1, 43(1)	
C		4 e 0 0 0.39522(5), 1, 67.2(9)	
distances/pm			
C−C		128.10(5)	
no. of refined param		40	
data range/Å	$0.6 \le d \le 8.2$	$0.5 \le d \le 4.2$	$0.6 \le d \le 3.2$
no. of reflections	104	156	92
R_p	0.0632	0.0625	0.0638
wR_p	0.0535	0.0393	0.0432
R_{Bragg}	0.0287	0.0168	0.0130

[a] Further details of this crystal-structure investigation may be obtained from the Fachinformationzentrum Karlsruhe, Eggenstein-Leopoldshafen, Germany, on quoting the depository number CSD 422605 (http://www.fiz-karlsruhe.de/).

Yb L_3 edge because of the $2p_{3/2}$ core hole lifetime.[9] Fitting of the spectra is often imprecise, especially if one valence state represents only a minor component. An improved resolution of the XANES spectra is therefore desirable to achieve more reliable information on the valence states in complex compounds. HERFD-XANES spectroscopy is the appropriate method in which a total spectral broadening of the Yb L_3 spectrum of ∼2.4 eV can be achieved.[10−16] A HERFD spectrum is recorded by monitoring the $L\alpha_1$ ($3d_{5/2}-2p_{3/2}$) intensity as a function of the incident energy with an instrumental energy bandwidth that is below the core hole lifetime broadening. The advantage of this technique is that the width of the spectral features is no longer limited by the $2p_{3/2}$ core hole lifetime but by the sharper $3d_{5/2}$ core hole width.

Complementary information about the valence state in dicarbide compounds can be obtained by analyzing the C−C bond length of the C_2 dumbbells. The occupancy of the conduction band in trivalent compounds results in a C−C distance of ∼129 pm (bonding order BO = 2.5) at room temperature,[4] whereas divalent compounds show a C−C distance of ∼120 pm (BO = 3.0) comparable to acetylene.[17] We therefore determined the C−C

dx.doi.org/10.1021/ic200247z |*Inorg. Chem.* 2011, 50, 5587–5595

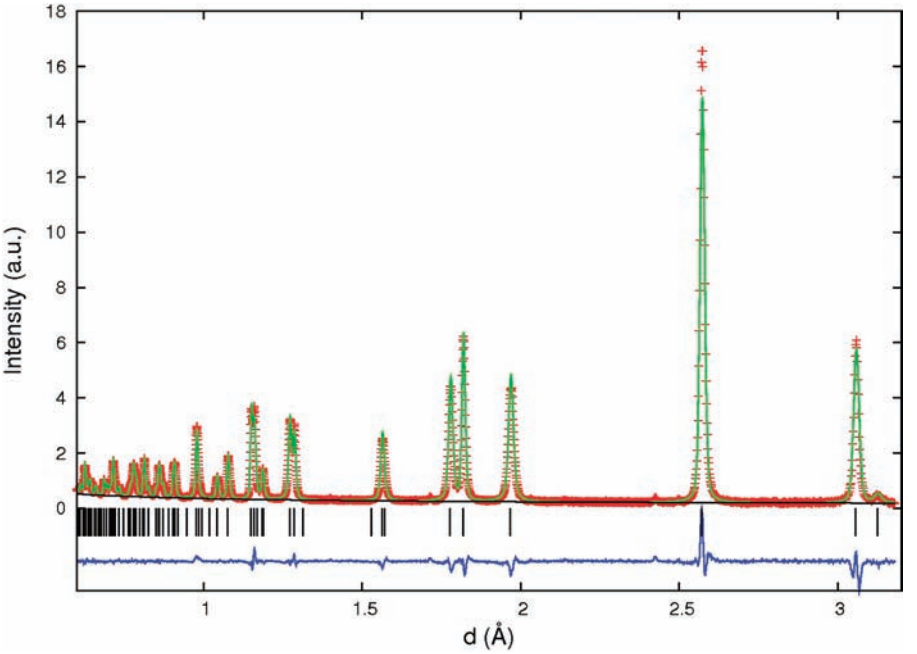

Figure 2. Rietveld refinement of a room temperature TOF powder neutron diffraction pattern of YbC_2 collected in the Polaris $2\theta \sim 145°$ detector bank. The experimental data points (red +), calculated profile (green line), calculated background (black line), and difference curve (blue line) are shown. The reflection positions are marked as black vertical bars.

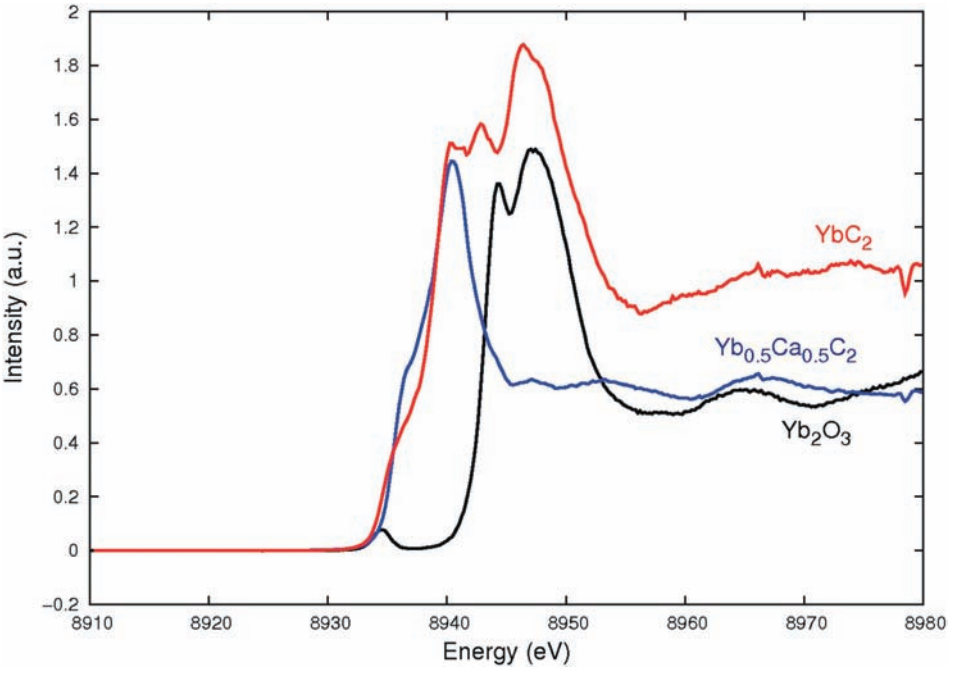

Figure 3. Yb L_3 HERFD-XANES spectra of YbC_2 (red), Yb_2O_3 (black), and $Yb_{0.5}Ca_{0.5}C_2$ (blue). The intensities in the spectra of Yb_2O_3 and $Yb_{0.5}Ca_{0.5}C_2$ were reduced to 60% to allow for a better comparison of the white lines.

bond length of YbC_2 from Rietveld refinements of time-of-flight (TOF) neutron powder diffraction data to support our results obtained from XANES spectroscopy.

EXPERIMENTAL SECTION

General Remarks. Because of the high sensitivity of Yb and YbC_2 to moisture and oxygen, all sample handling was carried out in an inert atmosphere (Ar, 99.999%). Yb metal pieces were obtained from Chempur (distilled, 99.99%) and filed to small chips in a glovebox (argon atmosphere). Prior to the reaction, graphite (Aldrich, 99.9998%) was heated to 1070 K for 48 h in a dynamic vacuum and stored in an argon atmosphere.

Sample Preparation. As described in the literature,[4,18] YbC_2 was synthesized by the direct reaction of the elements at high temperatures. In a typical reaction, 865.2 mg of Yb powder (5 mmol) and 123.1 mg of

dx.doi.org/10.1021/ic200247z |Inorg. Chem. 2011, 50, 5587–5595

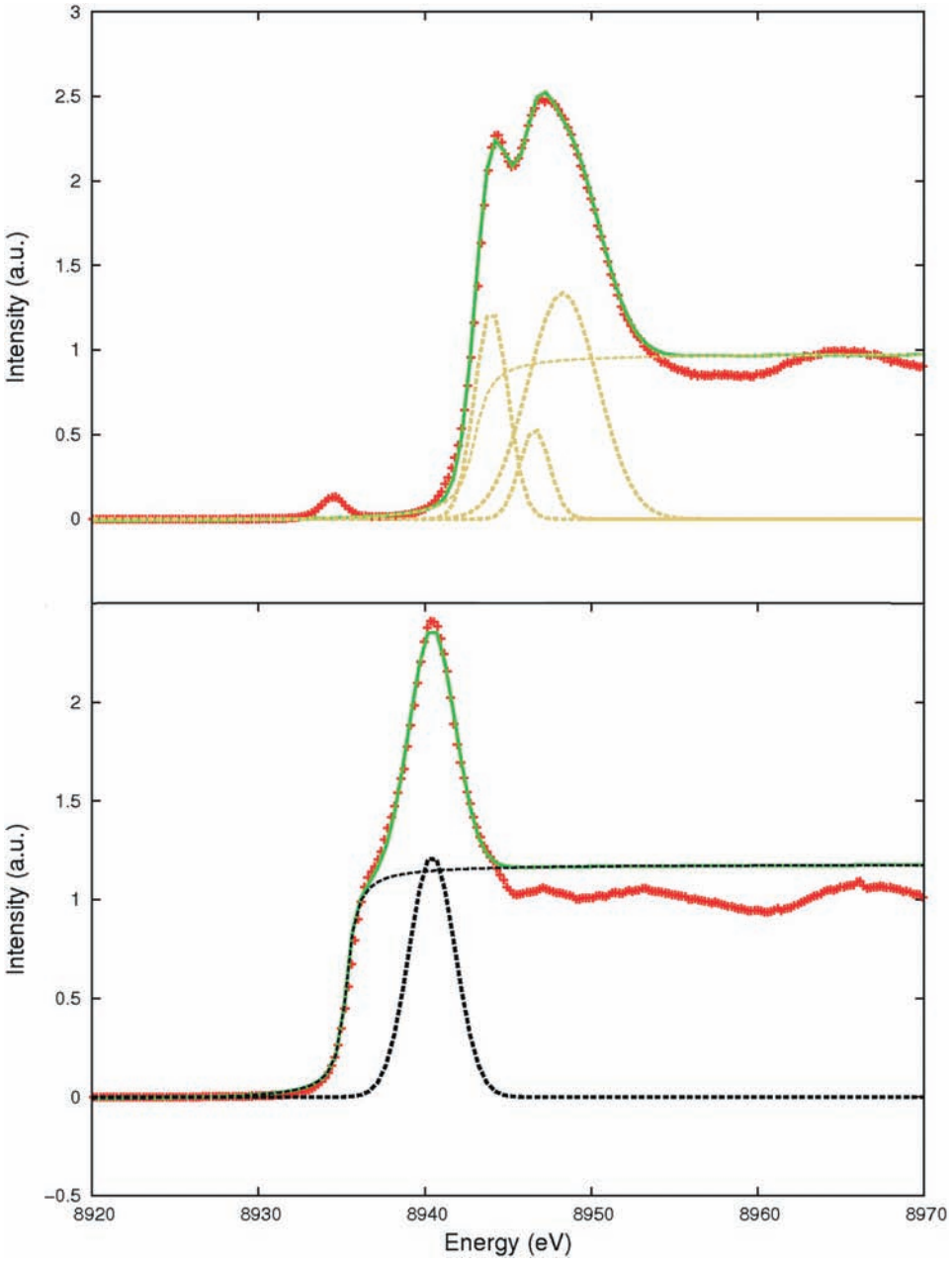

Figure 4. Least-squares fits of the Yb L_3 HERFD-XANES spectra of Yb_2O_3 (upper plot) and $Yb_{0.5}Ca_{0.5}C_2$ (lower plot). The experimental data are presented by red +, and the fitted spectrum is displayed in green. The components of the fit are shown as dotted lines.

graphite (10.25 mmol) were mixed in a shallow shell. A small surplus of graphite was chosen (Yb:C = 1:2.05) to inhibit the formation of Yb_2O_3 and account for graphite losses due to reactions with the container wall. The resulting mixture was transferred into a purified Ta ampule that was sealed in an arc furnace (helium atmosphere, 800 mbar, 10 A). The ampule was subsequently encapsulated into a silica tube under vacuum to avoid oxidation of the Ta metal at high temperatures. The resulting reaction container was heated in a high-temperature furnace (HTRH, GERO Hot Solutions) at 1323 K (heating rate of 250 K/h) for 24 h and cooled down by switching off the furnace. YbC_2 was obtained as a golden powder.

Structural Investigations. TOF neutron powder diffraction data were collected on the Polaris beamline at the ISIS pulsed spallation source (Rutherford Appleton Laboratory, Oxfordshire, U.K.).[19] Approximately 4.5 g of YbC_2 was loaded into a thin-walled cylindrical V sample can (diameter = 6 mm, height ≈ 50 mm, and wall thickness ≈ 0.15 mm) inside a glovebox (argon atmosphere), and the can was then sealed with In wire. Diffraction patterns were collected for ∼100 μAh (integrated proton beam current to the ISIS target, corresponding to a ∼40 min data collection time) at room temperature and also between 5 and 100 K in 5 K steps using an AS Scientific "orange" helium cryostat. The cryostat and sample can temperatures were monitored and controlled using RhFe temperature sensors connected to Eurotherm 3504 controllers. Data collected in three detector banks centered at $2\theta = 145°$ ($d_{max} = 3.2$ Å), $2\theta = 90°$ ($d_{max} = 4.2$ Å), and $2\theta = 35°$ ($d_{max} = 8.2$ Å) were normalized and corrected for absorption prior to crystal structure refinement. Full profile refinement by the Rietveld method was carried out with the *GSAS* sofware package.[20]

dx.doi.org/10.1021/ic200247z |*Inorg. Chem.* 2011, 50, 5587–5595

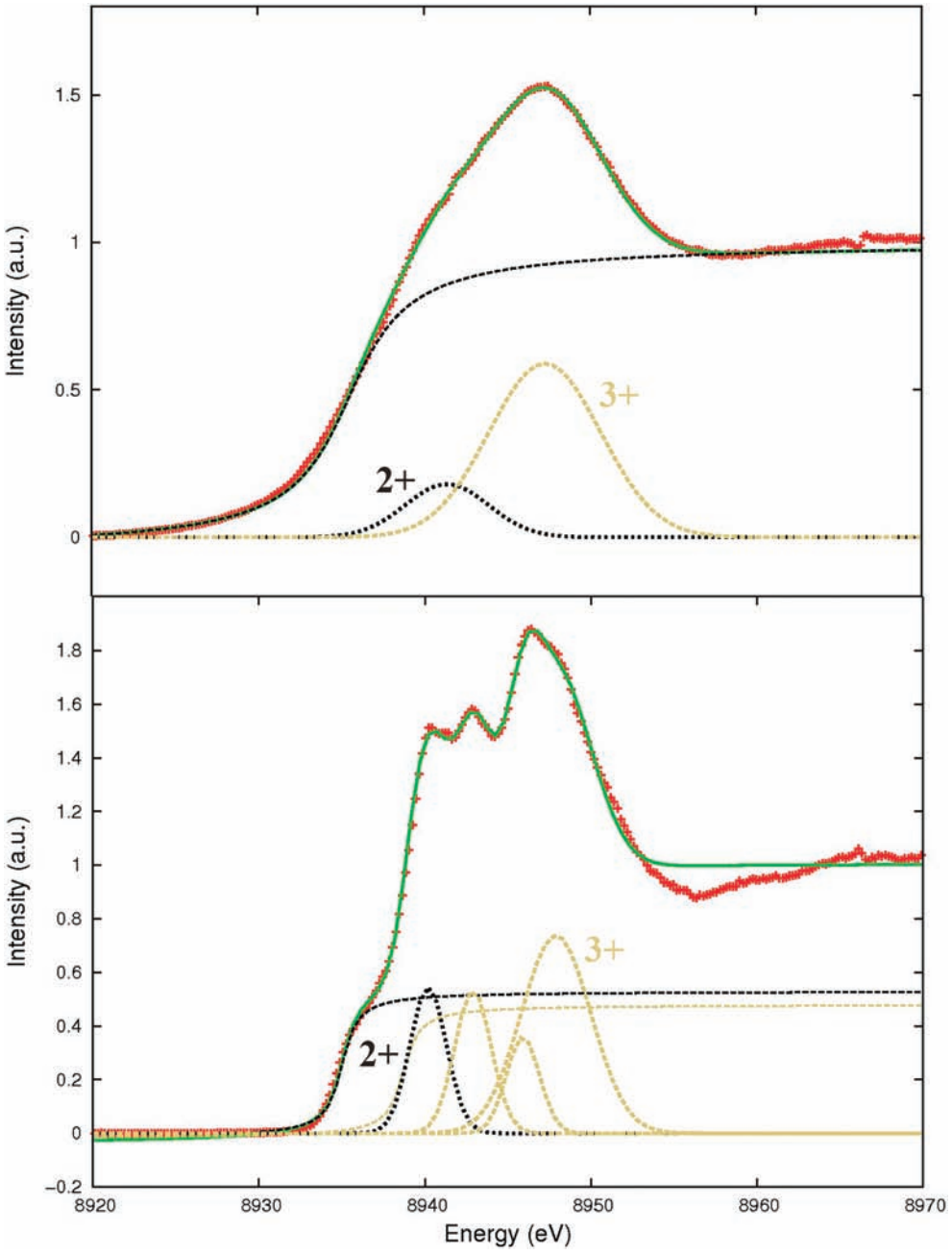

Figure 5. Least-squares fits of the Yb L_3 XANES spectra of YbC_2. The HERFD (lower plot) and TFY (upper plot) spectra are compared. The experimental data are presented by red +, and the fitted spectrum is displayed in green. The components of the fit are shown as dotted lines.

X-ray Spectroscopy. XANES spectra at the Yb L_3 edge were recorded at beamline ID26 of the European Synchrotron Radiation Facility (ESRF) in Grenoble, France.[21] The data were collected in fluorescence yield with high-energy-resolution (HERFD-XANES) using an X-ray emission spectrometer. The incident energy was selected using the ⟨311⟩ reflection from a double Si crystal monochromator. The incident flux was 5×10^{12} photons/s with a beam size on the sample of 1.0×0.1 mm^2 (horizontal × vertical). Subsequently, the fluorescence radiation of the sample was reflected by a Si ⟨620⟩ crystal analyzer, focusing the Yb $L\alpha_1$ line on a photon detector (avalanche photodiode). The sample, analyzer crystal, and detector were arranged in a vertical Rowland geometry. Conventional XANES spectra in total fluorescence yield (TFY) were detected simultaneously by using a photodiode. The intensity was normalized to the incident flux. Two different setups were used to collect data at low and high temperatures: (i) a closed-cycle helium cryostat for low-temperature investigations (15−300 K) and (ii) a high-temperature furnace for measurements between 300 and 1200 K. In both setups, temperature steps of 30 K were used. To achieve thermal equilibrium in all measurements, the samples were kept at the desired temperature for 15 min and subsequently measured for about 20 min. For the low-temperature measurements, samples were loaded in Lindemann glass capillaries (diameter = 0.5 mm), while quartz glass capillaries (diameter = 0.3 mm) were used for the high-temperature measurements. The capillaries were filled in a glovebox (argon atmosphere) and sealed airtight with a heated wire. All spectra were analyzed and normalized using the program *ATHENA* of the *IFEFFIT*

dx.doi.org/10.1021/ic200247z |*Inorg. Chem.* 2011, 50, 5587–5595

software package.[22] Subsequent least-squares fitting procedures were carried out with the program *GNUPLOT*.[23]

RESULTS

The neutron powder diffraction data collected at room temperature confirm the tetragonal crystal structure of YbC_2, which has already been described by several authors[4,24,25] (Table 1 and Figure 2). Thus, like most LnC_2 compounds, YbC_2 crystallizes in the CaC_2-type structure at room temperature. The refined lattice parameters agree well with the values published by Atoji,[4] Spedding et al.,[24] and Vickery et al.[25] within the accuracy of the refinement. The calculated C−C distance of 128.10(5) pm is again similar to the results of Atoji, who obtained a C−C distance of 128.7(9) pm from neutron diffraction experiments.[4] These values are comparable to those of other trivalent LnC_2 compounds, a finding that suggests an Yb valence of about 3+ for YbC_2. Our neutron powder pattern reveals a minor impurity phase that was identified as YbO. However, because the weight fraction of this oxide impurity is below 1%, it is neglected in the following discussion.

To determine the Yb valence as a function of the temperature, Yb L_3 HERFD-XANES spectroscopic experiments were carried out at beamline ID26 of the ESRF. The HERFD spectrum at room temperature compared to the spectra of the reference compounds Yb_2O_3 and $Yb_{0.5}Ca_{0.5}C_2$[26] is shown in Figure 3. Yb_2O_3 and YbC_2 show a pronounced splitting of the white lines that cannot be resolved in conventional TFY spectra. The splitting of the white line of trivalent Yb in Yb_2O_3 was first mentioned by Kvashnina et al. and reveals the fine structure of the 5d shell.[11] A detailed analysis of this splitting, which is also influenced by the crystal field, has recently been published for CeO_2 as a test case.[27] We found that with an empirical approach the white line in Yb_2O_3 may be described satisfactorily by three Gaussian functions (Figure 4, upper plot). However, the spectrum of $Yb_{0.5}Ca_{0.5}C_2$ containing only Yb^{2+} is well described with only one Gaussian function (Figure 4, lower plot). The spectrum of YbC_2 (Figure 5, lower plot) shows a white line at an energy of about 8946.5 eV with a splitting into three Gaussians that is even stronger than that of Yb_2O_3. In contrast to the oxide, a fourth peak can be observed at an energy of about 8940.2 eV, which apparently does not belong to the trivalent state of Yb. We, therefore, assigned this line to the divalent state (compare $Yb_{0.5}Ca_{0.5}C_2$, which only contains divalent Yb; Figure 4, lower plot). HERFD-XANES investigations on the dicarbide solid solution $Yb_xCa_{1-x}C_2$[26] confirm these assignments, as for low x spectra were obtained that exclusively contained a single line at 8940.2 eV without any fine structure splitting, whereas for high $x \approx 1$ spectra similar to YbC_2 were obtained. Hence, we can safely assume that the fourth line of YbC_2 is caused by divalent Yb, indicating a mixed-valence state. The pre-edge peak, caused by a 2p → 4f transition only observable in the case of trivalent Yb,[11] is found in the spectrum of Yb_2O_3 but not in that of YbC_2. Instead, the spectrum of YbC_2 contains a shoulder at the L_3 edge that is caused by the mixed valence of the compound.

On the basis of these considerations, we were able to carry out a least-squares fitting extracting the relative intensities of the two white lines. One Gaussian function was used to describe the divalent Yb state. The trivalent Yb state was described by three Gaussians, taking into account the fine structure splitting of the white line. Furthermore, two arctangent functions were used representing the L_3 edge and its shoulder. The average Yb valence was finally calculated by using the following formula:

$$\tilde{\nu} = 2 + \frac{I(\mathrm{Yb^{III}})}{I(\mathrm{Yb^{III}}) + I(\mathrm{Yb^{II}})}$$

where $I(\mathrm{Yb^{III}})$ and $I(\mathrm{Yb^{II}})$ are the integrated intensities (or spectral areas) of the respective valence states. The results of this fitting procedure compared to the fit of a conventional TFY spectrum is shown in Table 2. The quality of the fits can be seen in Figure 5. It is obvious that both methods result in the same average Yb valence of 2.81, which is, in our opinion, a good confirmation that the fitting approach for HERFD data that we have chosen leads to reliable results.[28] However, while the divalent white line is only visible as a small shoulder in the TFY spectrum and it can be clearly identified as a discrete peak in the HERFD spectrum, small changes in $\tilde{\nu}$ are detectable more accurately in HERFD experiments. Despite these promising results, it should be mentioned that edge shifts obtained in XANES spectroscopy should be interpreted as *relative* changes of the valencies or even better as changes of the electron densities on the absorber.

Table 2. Least-Squares Fitting Results of the HERFD and TFY XANES Spectra of Yb_2O_3 and $Yb_{0.5}Ca_{0.5}C_2$ (Reference Materials) and YbC_2 at Room Temperature

	function	E_{max}/eV	I/a.u.	fwhm/eV	$\tilde{\nu}$
		Yb_2O_3 (Reference, HERFD Method)			
edge	atan	8943.0(1)	1.03(1)	0.6(1)	3.0
Yb^{3+}	Gaussian	8944.0(1)	3.11(5)	1.05(2)	
		8946.6(2)	1.20(6)	0.91(4)	
		8948.3(1)	7.04(9)	2.09(3)	
		$Yb_{0.5}Ca_{0.5}C_2$ (Reference, HERFD Method)			
edge	atan	8935.3(2)	1.19(1)	0.45(8)	2.0
Yb^{2+}	Gaussian	8940.4(2)	4.2(2)	1.38(6)	
		YbC_2 (HERFD Method)			
edge	atan	8935.0(2)	0.55(2)	0.70(5)	2.81(6)
		8938.7(2)	0.50(2)	0.50(8)	
Yb^{2+}	Gaussian	8940.2(2)	1.50(4)	1.10(4)	
Yb^{3+}	Gaussian	8942.9(2)	1.47(4)	1.10(4)	
		8945.9(3)	0.90(4)	1.00(5)	
		8947.9(1)	3.88(6)	2.10(3)	
		YbC_2 (TFY Method)			
edge	atan	8935.5(1)	1.05(1)	2.68(5)	2.81(5)
Yb^{2+}	Gaussian	8941.4(2)	1.13(4)	2.50(9)	
Yb^{3+}	Gaussian	8947.3(1)	4.96(5)	3.36(4)	

The obtained valence value of 2.81 confirms the results of former investigations that have mainly been calculated from magnetization measurements.[4,5] However, our room temperature measurement does not contain any information about the type of mixed valence in YbC_2. The two different approaches of Atoji and Sales and Wohlleben mainly differ in the temperature dependence of the average Yb valence. While the *heterogeneous* model of Atoji should result in a temperature-independent valence, the *homogeneous* ICF model of Sales and Wohlleben predicts a strong decrease of the Yb valence with decreasing temperature down to 2.1 at $T = 0$ K. Thus, XANES spectroscopic investigations at high and low temperatures should be the appropriate tool to distinguish between the two models. Actually, we found no significant change of the Yb valence depending on

dx.doi.org/10.1021/ic200247z |*Inorg. Chem.* 2011, 50, 5587–5595

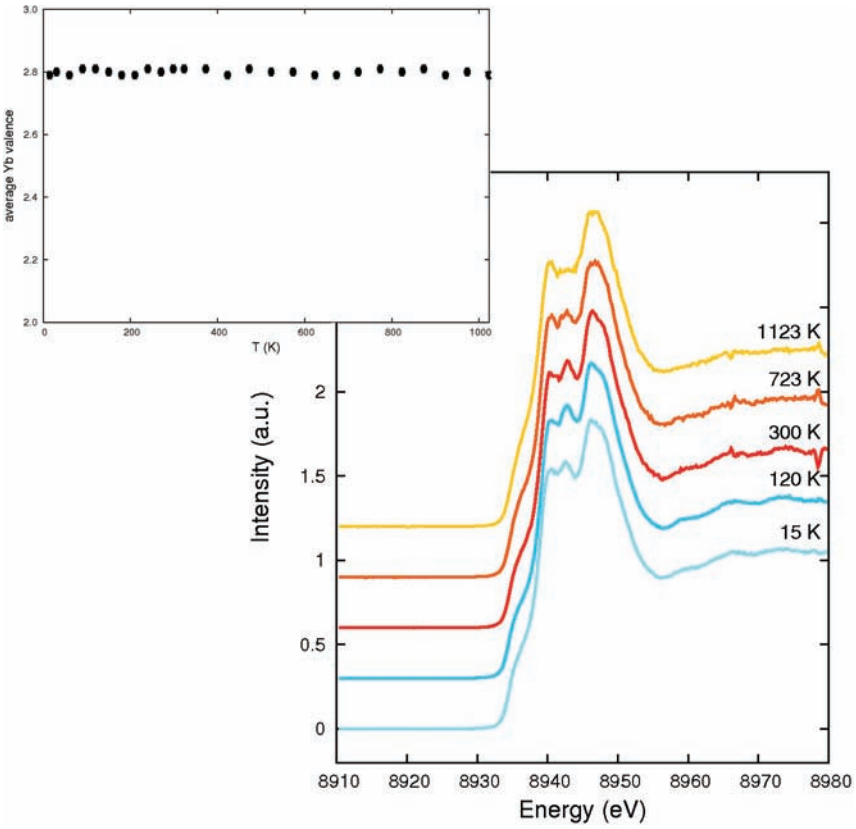

Figure 6. Yb L_3 HERFD-XANES spectra of YbC_2 at selected temperatures (right) and the average Yb valence, obtained by least-squares fitting of all measured spectra, as a function of the temperature (left).

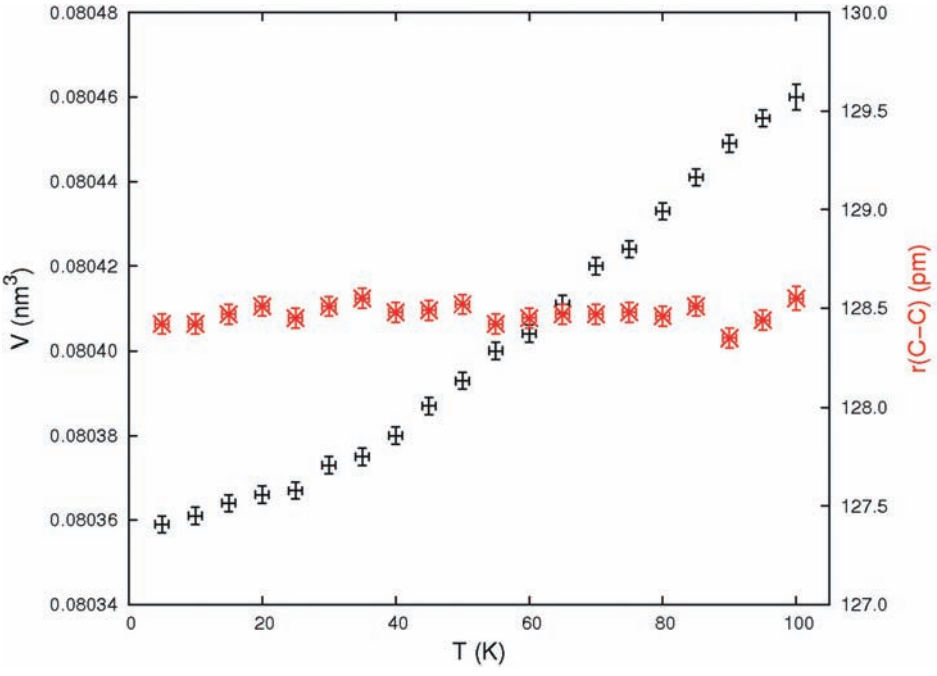

Figure 7. Unit cell volume (black dots) and the C−C distance (red crosses) of YbC_2 as a function of the temperature. The respective standard deviations are given.

the temperature. Down to 15 K, the HERFD spectra remain unchanged, and the predicted decrease of $\tilde{\nu}$ according to the model of Sales and Wohlleben could not be observed (Figure 6). The same behavior is observed for high temperatures up to 1123 K. No

dx.doi.org/10.1021/ic200247z |*Inorg. Chem.* 2011, 50, 5587–5595

significant changes of the white-line intensities were obtained during these measurements. The respective average Yb valence, calculated by least-squares fitting of all measured spectra, varies arbitrarily from 2.79 to 2.82, which is very close to the room temperature value of 2.81 (Figure 6).

These experimental findings are corroborated by neutron powder diffraction experiments at low temperatures. As mentioned above, the C−C distance in dicarbides may be used as an indicator for the valence state of the incorporated metal. A decrease of the Yb valence, as predicted by Sales and Wohlleben, should lead to a significant decrease of the C−C distance because the localization of the conduction electron causes a depopulation of the ligand π^* orbitals. Furthermore, a decreasing valence should increase the unit cell volume of the carbide because the ionic radius of the Yb^{2+} ion (R = 114 pm and CN = 8)[29] is much larger than the respective radius of Yb^{3+} (R = 99 pm and CN = 8).[29] Thus, one should expect a negative thermal expansion at low temperatures, which is, for example, observable in the fulleride $Yb_{2.75}C_{60}$.[30] As can be seen from Figure 7, the temperature-dependent unit cell volumes as well as the C−C distances in YbC_2 show an entirely "normal" behavior. The C−C bond length remains constant over the whole temperature range, while the unit cell volume exhibits a positive thermal expansion. This crystallographic information supports the results of our temperature-dependent XANES investigations. Both methods confirm a temperature-independent mixed Yb valence of 2.81 in YbC_2.

DISCUSSION

In the work reported here, we clearly revealed by Yb L_3 XANES spectroscopic investigations and TOF neutron powder diffraction experiments that YbC_2 contains Yb ions with a temperature-independent intermediate valence of ∼2.81. No significant change of the Yb valence was detected in the temperature range 15−1123 K. Our findings allow for a critical review of former work by Atoji and by Sales and Wohlleben, who obtained contrary results concerning the type of mixed valence in YbC_2.[4,5] Our XANES spectroscopic investigations disprove the results of Sales and Wohlleben, who derived a *homogeneous*, fluctuating valence state that was strongly temperature-dependent from analysis of the magnetization data. The results of Atoji seem to be in line with our experiments, as he derived a constant mixed valence from the Curie−Weiss behavior of the magnetic susceptibilities. A critical reexamination of the physical properties of YbC_2 is therefore strongly recommended to achieve complete characterization of this compound. First magnetization and electrical resistivity measurements have already been started in our group. The preliminary results suggest that the physical properties of YbC_2 are strongly influenced by impurities containing trivalent Yb, a reason that may explain the different results found in the literature. The magnetic susceptibilities seem to be more complex than described by Atoji, but further investigations are needed to allow a reliable interpretation of these data. In addition, supporting experiments like ^{170}Yb Mössbauer spectroscopy should be used to confirm the results of our empirical fitting approach and to clearly differentiate between *homogeneous* and *heterogeneous* mixed-valence behavior. Because the chemical shift difference $\Delta\delta$ between the divalent and trivalent states of Yb is very small in ^{170}Yb Mössbauer spectra, the strongly varying quadrupole splittings of both states may be used to quantify the averaged valence of the Yb ion.[31] Because of its totally filled 4f shell, the divalent state exhibits a very small quadrupole splitting $\Delta E_Q \approx 4$ mm/s, whereas the $4f^{13}$ state of trivalent Yb produces a large splitting of $\Delta E_Q \approx 30$ mm/s.[31,32] A dynamic valence fluctuation may be identified by the occurrence of a single spectral component rather than two distinct components in the case of a *heterogeneous* mixed-valence state.[32] Unfortunately, ^{170}Yb Mössbauer spectroscopy is not as common as ^{151}Eu spectroscopy because the ^{170}Yb isotope only accounts for 3% of the natural Yb sources. However, some work has been published recently that presents results using ^{170}Yb Mössbauer spectroscopy in Yb systems with unusual valences.[32−34] Thus, ^{170}Yb Mössbauer experiments will be part of our future investigations on YbC_2 to clarify the nature of its mixed Yb valence.

The intermediate valence in YbC_2 suggests that it should be possible to manipulate the Yb valence state by external factors. Therefore, we studied the impact of "chemical pressure" on the Yb valence by synthesizing solid solutions $Yb_xEA_{1-x}C_2$, composed of YbC_2 and an alkaline-earth metal dicarbide EAC_2 (with EA = Ca, Sr, and Ba).[26] Indeed, we found interesting valence effects in these systems, and these will be presented in the near future.

In conclusion, we have shown that YbC_2 possesses an intermediate Yb valence of ∼2.81 that is temperature-independent from 15 to 1123 K. However, it has to be clarified whether the mixed-valence state is *homogeneous* or *heterogeneous*. This question shall be solved by ^{170}Yb Mössbauer spectroscopy in the near future. As a consequence of our findings, the physical properties of YbC_2 have to be reinvestigated to obtain a complete picture of this long-known compound.

ASSOCIATED CONTENT

Supporting Information. Crystallographic data in CIF format. This material is available free of charge via the Internet at http://pubs.acs.org.

AUTHOR INFORMATION

Corresponding Author
*E-mail: Uwe.Ruschewitz@uni-koeln.de.

ACKNOWLEDGMENT

We are grateful to the technical support staff at ESRF for assistance during the experiment. Experiments at the ISIS Pulsed Neutron and Muon Source were supported by a beamtime allocation from the Science and Technology Facilities Council. We thank the German Research Foundation for financial support (Grants SPP 1166 and RU 546/8-1).

REFERENCES

(1) Vickery, R. C.; Sedlacek, R.; Ruben., A. *J. Chem. Soc.* **1959**, 503–505.
(2) Sakai, T.; Adachi, G.; Yoshida, T.; Shiokawa, J. *J. Chem. Phys.* **1981**, *75*, 3027–3032.
(3) Wandner, D.; Link, P.; Heyer, O.; Mydosh, J.; Ahmida, M. A.; Abd-Elmeguid, M. M.; Speldrich, M.; Lueken, H.; Ruschewitz, U. *Inorg. Chem.* **2010**, *49*, 312–318. *Inorg. Chem.* **2011**, *50*, 2703.
(4) Atoji, M. *J. Chem. Phys.* **1961**, *35*, 1950–1960.
(5) Sales, B. C.; Wohlleben, D. K. *Phys. Rev. Lett.* **1975**, *35*, 1240–1244.
(6) Heim, H.; Bärnighausen, H. *Acta Crystallogr., Sect. B* **1978**, *34*, 2084–2092.
(7) Sankar, G.; Sarode, P. R.; Rao, C. N. R. *Chem. Phys.* **1983**, *76*, 435–442.

(8) Centeno, M. A.; Malet, P.; Carrizosa, I.; Odriozola, J. A. *J. Phys. Chem. B* **2000**, *104*, 3310–3319.
(9) Fuggle, C.; Inglesfield, J. E. *Top. Appl. Phys.* **1992**, *69*, 1–23.
(10) de Groot, F. M. F.; Krisch, M. H.; Vogel, J. *Phys. Rev. B* **2002**, *66*, 195112/1–195112/7.
(11) Kvashnina, K. O.; Butorin, S. M.; Glatzel, P. *J. Anal. At. Spectrom*. **2011**, DOI: 10.1039/C0JA00142B.
(12) Swarbrick, J. C.; Skyllberg, U.; Karlsson, T.; Glatzel, P. *Inorg. Chem.* **2009**, *48*, 10748–10756.
(13) Dallera, C.; Grioni, M.; Shukla, A.; Vankó, G.; Sarrao, J. L.; Rueff, J.-P.; Cox, D. L. *Phys. Rev. Lett.* **2002**, *88*, 196403/1–196403/4.
(14) Dallera, C.; Wessely, O.; Colarieti-Tosti, M.; Eriksson, O.; Ahuja, R.; Johansson, B.; Katsnelson, M. I.; Annese, E.; Rueff, J.-P.; Vankó, G.; Braicovich, L.; Grioni, M. *Phys. Rev. B* **2006**, *74*, 081101/1–081101/4.
(15) Dallera, C.; Annese, E.; Rueff, J. P.; Palenzona, A.; Vankó, G.; Braicovich, L.; Shukla, A.; Grioni, M. *J. Electron Spectrosc. Relat. Phenom.* **2004**, *137*−*140*, 651–655.
(16) Annese, E.; Rueff, J.-P.; Vankó, G.; Grioni, M.; Braicovich, L.; Degiorgi, L.; Gusmeroli, R.; Dallera, C. *Phys. Rev. B* **2004**, *70*, 075117/1–075117/6.
(17) Vohn, V.; Kockelmann, W.; Ruschewitz, U. *J. Alloys Compd.* **1999**, *284*, 132–137.
(18) Haschke, J. M.; Eick, H. A. *J. Am. Chem. Soc.* **1970**, *92*, 1526–1530.
(19) Hull, S.; Smith, R. I.; David, W. I. F.; Hannon, A. C.; Mayers, J.; Cywinski, R. *Physica B* **1992**, *180 & 181*, 1000–1002.
(20) Larson, A. C.; Dreele, R. B. Los Alamos National Laboratory Report LA-UR-86-748, 1987.
(21) Gauthier, C.; Solé, V.; Signorato, R.; Goulon, J.; Moguiline, E. *J. Synchrotron Radiat.* **1999**, *6*, 164–166.
(22) Newville, M. *IFEFFIT*, version 1.2.11c; University of Chicago: Chicago, IL, 2008.
(23) *GNUPLOT*, version 4.4.0; open source.
(24) Spedding, F. H.; Gschneidner, K., Jr.; Daane, A. H. *J. Am. Chem. Soc.* **1958**, *80*, 4499–4503.
(25) Vickery, R. C.; Sedlacek, R.; Ruben, A. *J. Chem. Soc.* **1959**, 498–502.
(26) Link, P.; Ruschewitz, U. *Z. Anorg. Allg. Chem.* **2008**, *634*, 2060. A more detailed publication is in preparation.
(27) Kvashnina, K. O.; Kotani, A.; Butorin, S. M.; Glatzel, P. **2011**, submitted for publication.
(28) Because , from a theoretical point of view, no clear approach for the fitting of HERFD spectra at Yb L_3 is given, the procedure given above is only one possible way. Other fitting procedures have also been attempted. They result in the same (qualitative) trends, but the resulting valence of Yb might differ by 0.15 units.
(29) Lide, D. R. *CRC Handbook of Chemistry and Physics*, 81st ed.; CRC Press: Boca Raton, FL, 2000.
(30) Margadonna, S.; Arvanitidis, J.; Papagelis, K.; Prassides, K. *Chem. Mater.* **2005**, *17*, 4474–4478.
(31) Ryan, D. H.; Cadogan, J. M. *Hyperfine Interact.* **2004**, *153*, 43–55.
(32) Mazet, T.; Ihou-Mouko, H.; Ryan, D. H.; Voyer, C. J.; Cadogan, J. M.; Malaman, B. *J. Phys.: Condens. Matter* **2010**, *22*, 116005/1–116005/13.
(33) Saensunon, B.; Nishimura, K.; Voyer, C. J.; Ryan, D. H.; Hutchison, W. D.; Stewart, G. A. *J. Appl. Phys.* **2009**, *105*, 07E123/1–07E123/3.
(34) Dhar, S. K.; Manfrinetti, P.; Fornasini, M. L.; Bonville, P. *Eur. Phys. J. B* **2008**, *63*, 187–192.